CHILEAN JOURNAL of AGRICULTURAL RESEARCH

RESEARCH ARTICLE

Geostatistical analysis of fall armyworm damage and edaphoclimatic conditions of a mosaic of agroecosystems predominated by push-pull systems

Ouorou Ganni Mariel Guera[1, 2*], Federico Castrejón-Ayala[1], Norma Robledo[1], Alfredo Jiménez-Pérez[1], Van-Huong Le[3], Martín Alberto Díaz-Viera[4], and José Antônio Aleixo da Silva[5]

[1]Instituto Politécnico Nacional (IPN), Centro de Desarrollo de Productos Bióticos, Yaupetec, Morelos, México.
[2]Universidad Politécnica del Estado de Morelos (UPEMOR), Morelos, México.
[3]University of Wyoming (UW), Laramie, Wyoming, USA.
[4]Universidad Nacional Autónoma de México (UNAM), Instituto Mexicano de Petróleo (IMP), México.
[5]Universidade Federal Rural de Pernambuco (UFRPE), Departamento de Ciência Florestal, Recife, Brasil.
[*]Corresponding author (gguerao1800@alumno.ipn.mx).

Received: 3 May 2022; Accepted: 7 July 2022; doi: 10.4067/S0718-58392023000100014

ABSTRACT

Some agroecological pest management systems manipulate insect behavior. The push-pull systems are the most functional implemented, reducing the insect-pest density and modifying its distribution. The present work analyzed the spatial distribution of incidence and severity of fall armyworm (FAW) (*Spodoptera frugiperda* (J.E. Smith), Lepidoptera: Noctuidae), and soil moisture and temperature in maize (*Zea mays* L.) crops of a mosaic of agroecosystems predominated by push-pull systems established in Yautepec, Morelos, Mexico. Univariate and multivariate spatial estimates were performed by geostatistical analysis applying ordinary kriging and cokriging, respectively. The results indicated that FAW incidence and severity presented an aggregated spatial distribution and soil moisture and temperature, a more continuous distribution. The estimated spatial distributions in the third week indicated that FAW incidence in push-pull systems varied between 10% and 40%, and in maize monocultures, between 35% and 90%. Fall armyworm damage severity ranged between 20% and 70% in monocultures and between 1% and 25% in the push-pull systems.

Key words: Cokriging, fall armyworm incidence and severity, kriging, soil temperature and moisture, *Spodoptera frugiperda*.

INTRODUCTION

Spodoptera frugiperda (J.E. Smith) (Lepidoptera: Noctuidae) is a polyphagous insect that feeds on plants of 353 species belonging to 76 families (Montezano et al., 2018). This generalist habit allows it to colonize various agroecosystems with an unpredictable spatial-temporal distribution. Furthermore, this distribution may change with the impact of climate change (Bebber et al., 2013). Therefore, knowing the pest distribution is of utmost importance for the correct application of control measures and management strategies (Prá et al., 2011). The information provided by the spatial distribution is also helpful in improving the efficiency and precision of pest sampling (Davis, 1994).

Among the techniques used to study pest distribution, geostatistics stands out (Farias et al., 2008). Geostatistical analysis is applied to study of agroecosystems as one of the recommended precision agriculture techniques. At present, agroecological systems are probably the most complex. Their study generates a large volume of data whose analysis requires advanced statistical techniques that include aspects not considered by classical statistics, among others, spatial variation. The classical statistical methods consider the spatial variations as part of the random errors. In the design of experiments, mainly those in the field, Sir Ronald A. Fisher proposed

using large plots to reduce the effect of short-range spatial variation and blocks to control long-range spatial variation (Oliver, 2010). However, in agricultural experiments, the spatial variation of certain variables such as edaphic or phytosanitary, whose spatial dependence is well known, cannot always be controlled through these recommendations (Pringle et al., 2010).

Geostatistics is the primary technique used to analyze experiments in a spatially explicit context (Cressie, 1993; Pringle et al., 2010). Its use allows the control and better management of agricultural pests (Dminić et al., 2010). It provides a valuable information to understand the determining factors of pest population dynamics (Liebhold et al., 1993). These dynamics are studied by comparing maps interpolated at different times to detect changes or persistence in spatial patterns over time (Goovaerts and Chiang, 1993). The study of fall armyworm (FAW) spatial distribution is essential to determine its distribution patterns and population growth rates to develop monitoring strategies and control the insect pest populations and therefore reduce maize yield losses (Hutasoit et al., 2020).

Agriculture is also influenced by climate, soil, and water (Talchabhadel et al., 2019). In an agroecosystem, the main water management subsystem is soil. Soil moisture and temperature are the two most important variables for crop growth, development, and yield formation (Zhang et al., 2020). According to Brevik et al. (2016), mapping is one of the main methods for understanding these soil characteristics. Spatial information on these characteristics is essential for correct decision-making (Lopes and Montenegro, 2019). Soil water content depends on its type, climatic conditions, and water supply (Azizan et al., 2019), while its spatial distribution depends on the joint action of its properties, presence, type, vegetation density, and meteorological conditions (Famiglietti et al., 1998). Soil temperature influences several metabolic processes of plants (Al-Kayssi et al., 1990). Its rise generally increases mineral absorption by plants and accelerates their growth (Gosselin and Trudel, 1986). Knowing the spatial distribution of these soil characteristics is essential for decision-making to improve agricultural productivity and the sustainability of agroecosystems.

In this context, the present work reports our findings on the spatial distribution of soil moisture and temperature and FAW incidence and severity in maize crops of a mosaic of agroecosystems predominated by push-pull systems established in Yautepec, Morelos, Mexico.

MATERIALS AND METHODS

The present study was conducted in the mosaic of agroecosystems established in the field effectiveness evaluation experiment conducted by Guera et al. (2021) in an area located between coordinates 18.893323N and 99.102158W. This mosaic consists of the treatments evaluated in the experiment (Table 1): monocultures (negative control) and nine push-pull systems proposed by Guera et al. (2020). During the experimental period from June to December 2019, mean temperature was 23.61 ± 8.68 °C, and relative humidity was 75.01 ± 23.68%.

Table 1. Treatments evaluated in field effectiveness experiment conducted in Yautepec, Morelos, Mexico. [1]Trap plants established at a distance around the main crop (maize). [2]Plants intercropped in the main crop (maize). Source: Guera et al. (2021).

Nr	Treatments	Components	
		Attractants[1]	Intercrops[2]
1	MIIC	*Brachiaria hybrid* 'Mulato II'	*Crotalaria juncea* L.
2	MIIT		*Tagetes erecta* L.
3	MIID		*Dysphania ambrosioides* (L.) Mosyakin & Clemants
4	MC	*Panicum maximum* 'Mombasa'	*C. juncea*
5	MT		*T. erecta*
6	MD		*D. ambrosioides*
7	TC	*Panicum maximum* 'Tanzania'	*C. juncea*
8	TT		*T. erecta*
9	TD		*D. ambrosioides*
10	M	Maize monoculture not treated with pesticides (negative control)	

Data preparation and geostatistical analysis

The data used are from maize (*Zea mays* L.) cultivation areas (10 m × 10 m) of 30 experimental plots (14 m × 14 m) established in a randomized complete block design (RCBD) (Guera et al., 2021). All variables were sampled using the five-gold method in each plot. Soil temperature and moisture were measured after canopy closure in maize crops, 2 mo after their establishment, after a mid-summer drought of approximately 2 wk. The fall armyworm (FAW) (*Spodoptera frugiperda* (J.E. Smith), Lepidoptera: Noctuidae) incidence was measured at 7 (FAI1), 14 (FAI2), and 21 (FAI3) d and the severity at 21 d, reviewing 10 maize plants in each point of the five-gold sampling system established in each experimental plot. A total of 150 points were georeferenced by their UTM geographic coordinates surveyed with a GPS (eTrex 10, Garmin, Kansas City, Kansas, USA).

Geostatistical analysis is divided into three main stages: exploratory analysis, variographic analysis, and spatial estimation (Figure 1). In the exploratory analysis, basic statistics (measures of central tendency, dispersion, and shape) and graphs (histograms and boxplots) were used to describe the statistical behavior of variables under study. The variables whose data did not attend symmetric and mesokurtic distribution were subjected to transformations determined by the Box-Cox family of transformations (Box and Cox, 1964) (Equation 1). The presence of distributional outliers was also verified by the method adopted by Díaz-Viera et al. (2021):

$$W_{(\lambda)} = \begin{cases} Ln(Y), & si\ \lambda = 0 \\ \dfrac{y^{\lambda} - 1}{\lambda}, & si\ \lambda \neq 0 \end{cases} \quad (1)$$

where, $W_{(\lambda)}$ is the transformed variable; y is the original variable and λ is the transformation coefficient that maximizes maximum likelihood estimator and minimizes residuals.

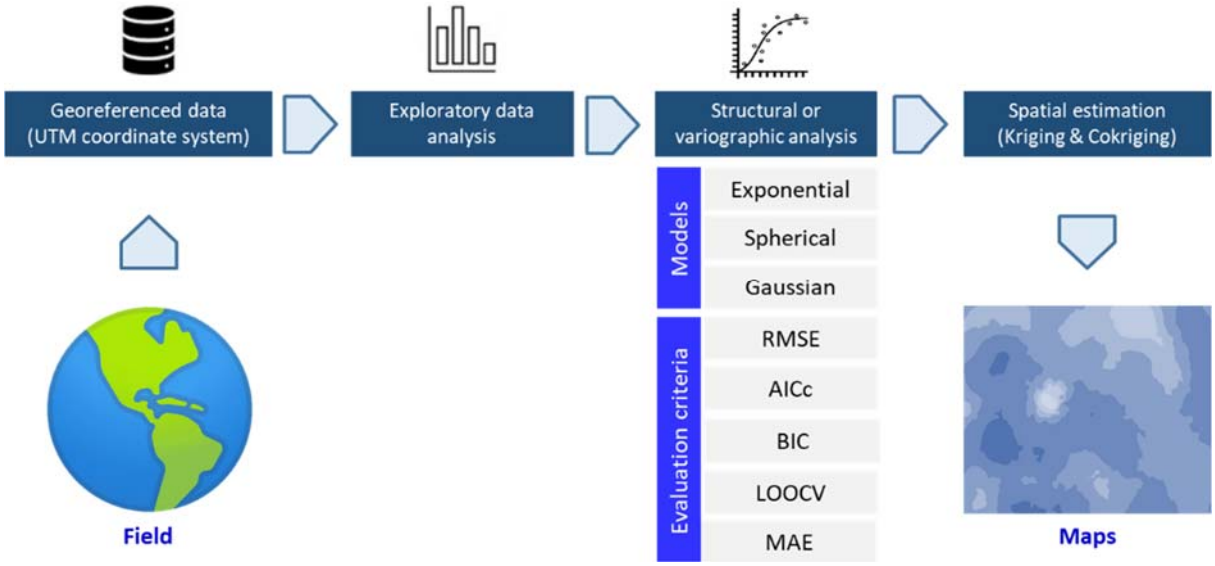

Figure 1. Geostatistical analysis stages.

Variographic analysis

This stage consisted of semivariograms estimation in the directions 0°, 45º, 90º, and 135º with angular tolerance of ± 22.5° to verify the presence of anisotropy. The experimental semivariograms were estimated using variogram and cross variogram formulas proposed by Matheron (1963). The theoretical variogram models of Table 2 were fitted to experimental variograms (scatter points). Each model indicates a different spatial pattern. The spherical model is appropriate for abrupt changes, the exponential describes relatively irregular phenomena, and the Gaussian is adopted for regular and continuous phenomena (Teixeira et al., 2012):

$$\hat{\gamma}(h) = \frac{1}{2N(h)} \sum_{i=1}^{n(h)} [Z_1(x_i) - Z_1(x_i + h)]^2 \quad (2)$$

$$\hat{\gamma}(h_{1,2}) = \frac{1}{2N(h)} \sum_{i=1}^{n(h)} [Z_1(x_i) - Z_1(x_i + h)][Z_2(x_i) - Z_2(x_i + h)] \quad (3)$$

where, $\hat{\gamma}(h)$ is semivariance estimate; N(h) is the number of pairs of measured values $Z(x_i)$ and $Z(x_i + h)$ separated by a vector h; Z_1 is the primary variable and Z_2 is the secondary variable.

Table 2. Theoretical variogram models. γ(h): Semi-variance; h: lag distance; C_0: nugget effect; R: range (the distance at which the variogram reach the sill); $C_0 + C_1$ sill (the value where the variogram model reaches a plateau and stabilizes).

Models	Mathematical expressions
Exponential	$\gamma(h) = \begin{cases} C_0 & \lvert h\rvert = 0 \\ C_0 + C_1\left[1 - exp\left(-\frac{3\lvert h\rvert}{R}\right)\right] & \lvert h\rvert \neq 0 \end{cases}$
Spherical	$\gamma(h) = \begin{cases} C_0 & \lvert h\rvert = 0 \\ C_0 + C_1\left[\frac{3}{2}\left(\frac{\lvert h\rvert}{R}\right) - \frac{1}{2}\left(\frac{\lvert h\rvert}{R}\right)^3\right] & 0 < \lvert h\rvert \leq R \\ C_0 + C_1 & \lvert h\rvert > R \end{cases}$
Gaussian	$\gamma(h) = \begin{cases} C_0 & \lvert h\rvert = 0 \\ C_0 + C_1\left[1 - exp\left\{-3\left(\frac{\lvert h\rvert}{R}\right)^2\right\}\right] & \lvert h\rvert \neq 0 \end{cases}$

The best model for each variable was selected through cross-validation, the corrected Akaike information criterion (AICc) (Equations 4 and 5), and the Bayesian information criterion (BIC) (Equation 6). The degree of spatial dependence (DSD) was analyzed by the ratio between the nugget effect (C_0) and the plateau ($C_0 + C_1$) and interpreted based on the following classification (Cambardella et al., 1994): Strong (DSD < 25%), moderate (25 < DSD ≤ 75%) and weak (DSD > 75%):

$$AIC_c = AIC + \frac{2k(k+1)}{n-k-1} \quad (4)$$

$$AIC = n \ln\left(\frac{SSE}{n}\right) + 2k \quad (5)$$

$$BIC = n \ln\left(\frac{SSE}{n}\right) + k \ln(n) \quad (6)$$

where, AIC is Akaike information criterion; k is number of parameters; n is number of observations; SSE is sum of squared estimate of errors.

The leave-one-out cross-validation (LOOCV) procedure was used to evaluate the model's performance. This procedure consists of estimating the value of a withdrawn observation with the rest of the observations. The process is repeated with each observation. The error of each estimate is the difference between its value and the observed one (Z - Z*) and is calculated using the expression 7. The best fit models are those with a mean absolute error (Equation 8), a mean squared error (Equation 9), and a root mean square error (Equation 10) closer to zero:

$$\varepsilon_i = Z(\underline{x}_i) - Z^*(\underline{x}_i) \qquad i = 1, \ldots, n \quad (7)$$

$$MAE = \frac{1}{n}\sum_{i=1}^{n} Z(\underline{x}_i) - Z^*(\underline{x}_i) \quad (8)$$

$$MSE = \frac{1}{n}\sum_{i=1}^{n} \left[Z(\underline{x}_i) - Z^*(\underline{x}_i)\right]^2 \quad (9)$$

$$RMSE = 100 \sqrt{\frac{\sum_{i=1}^{n} \left[Z(\underline{x}_i) - Z^*(\underline{x}_i)\right]^2}{n}} \Big/ \bar{Z} \quad (10)$$

where, ε_i is error associated with estimation of observation i, MAE is mean absolute error, MSE is mean squared error, RMSE is root mean square error, Z is observed value, Z* is estimated value and $\bar{Z}$ is the mean of observed values.

Spatial estimation

The fitted variogram models are used to interpolate all variables with the kriging method, which is a linear unbiased estimator. While FAW severity and soil moisture were interpolated with the cokriging method, which is a generalization of the kriging method for the multivariate case. Both methods use spatial autocorrelation to determine the coefficients of the estimator, but cokriging also considers the correlation between the variables (Chilès and Delfiner, 2012). With the interpolations, thematic maps were made to appreciate changes or persistence of spatial patterns in the distribution of FAW incidence/severity and soil temperature/moisture in the studied area. All analyses were performed in R 4.0.2 (R Foundation for Statistical Computing, Vienna, Austria).

RESULTS AND DISCUSSION

Exploratory data analysis

The descriptive analysis and the correlation matrix of the data referring to fall armyworm (FAW) incidence and severity and soil temperature and moisture in maize crops are summarized in Table 3 and Figure 2, respectively. As expected, a significant positive correlation was observed between FAW incidences in the first 3 wk and FAW severity in the third week. The FAW incidence at the third week (FAI3) was the most associated with FAW severity (FAS). Like the phytosanitary variables and the results of Al-Kayssi et al. (1990), a positive correlation was observed between soil moisture (Msoil) and temperature (Tsoil).

The results indicate that FAI1 presents a symmetric distribution, FAI2 an approximately symmetric distribution, FAI3, and FAS strong positive skewness, Msoil a strong negative skewness, and Tsoil a moderate positive skewness. Regarding kurtosis, FAI1, FAI2, and Tsoil presented mesokurtic distributions, Msoil a moderately leptokurtic distribution, and FAI3 and FAS highly leptokurtic distributions (Table 3).

Except for Tsoil and Msoil, all variables presented a high coefficient of variation (> 40%), the highest value being recorded in FAS. The logarithmic transformation was applied to FAI3, FAS, Msoil, and Tsoil. In the last two, it was necessary to remove outliers before applying the logarithmic transformation to obtain the desired distributions. Data ready for variographic analysis are in Figures 3 and 4.

Variographic analysis

The directional semivariograms of each variable were calculated in the directions 0°, 45°, 90°, and 135°, with an angular tolerance of ± 22.5°. All variograms were estimated with a lag increment of 4.208 m, resulting in 15 lags. The discrepancies in the ranges and sills were slight, which indicates the absence of anisotropy. So, we proceeded to compute experimental isotropic semivariograms and their subsequent adjustment to the theoretical models. In all the omnidirectional semivariograms (Figure 5), it was observed that the difference between the values of the variables increases as the distance increases until it reaches a relatively constant value. This result indicates that at least the intrinsic hypothesis is fulfilled. The error maps (Z - Z*) resulting from the leave-one-out cross-validation (LOOCV) method are found in Figure 6. All models presented mean errors close to zero, indicating the absence of bias in their estimates.

Table 3. Results of the descriptive statistical analysis of georeferenced data. FAI1: Fall armyworm (FAW) incidence at 7 d; FAI2: FAW incidence at 14 d; FAI3: FAW incidence at 21 d; FAS: FAW severity at 21 d; Msoil: soil moisture; Tsoil: soil temperature; SD: standard deviation; CV: coefficient of variation.

Variables	FAI1	FAI2	FAI3	FAS	Msoil	Tsoil
Minimum	0.000	0.000	10.000	1.250	40.000	19.440
1st quartile	10.000	20.000	20.000	5.000	72.000	24.027
Median	20.000	30.000	30.000	8.750	78.000	25.560
Mean	19.133	25.400	31.067	13.508	75.487	25.915
3rd quartile	27.500	30.000	37.500	16.250	80.750	27.082
Maximum	40.000	60.000	90.000	67.500	92.000	33.330
SD	8.969	10.273	14.662	13.201	9.440	2.611
CV	46.877	40.445	47.195	97.727	12.510	10.080
Skewness	-0.053	-0.451	1.571	1.787	-1.190	0.528
Kurtosis	2.689	3.544	6.069	6.132	4.759	3.438

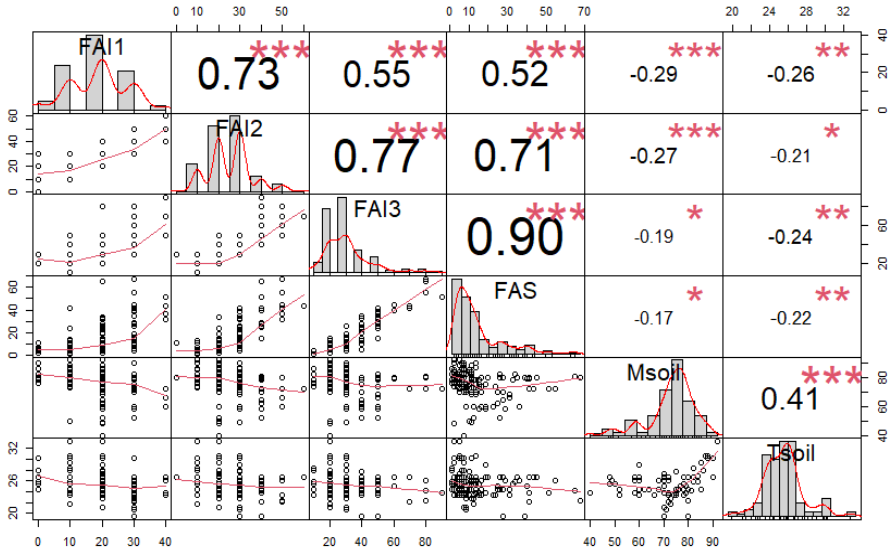

Figure 2. Correlation matrix for all pairs of the observed variables (read from the diagonal). The lower part shows scatter plots and smoothing splines for each possible pair; the upper part shows the Pearson correlation coefficient (text size proportional to absolute value). The significance of the correlation coefficients at different levels is indicated by the following symbols: 0.05 (*), 0.01 (**) and 0.001 (***). FAI1: Fall armyworm (FAW) incidence at 7 d; FAI2: FAW incidence at 14 d; FAI3: FAW incidence at 21 d; FAS: FAW severity at 21 d; Msoil: soil moisture; Tsoil: soil temperature.

The experimental semivariograms indicate spatial dependence in the analyzed variables (Figure 5). The spherical model was better fitted to the phytosanitary variables and the Gaussian to the edaphoclimatic variables (Table 4). This result agrees with those of Ramírez-Dávila et al. (2002), according to which the spherical model is recommended to interpolate plants harmful agents, and Farias et al. (2008), for whom the most representative model for FAW spatial dependence was also the spherical one. The adjustment of the spherical model to incidence (FAI1, FAI2, and FAI3) and severity (FAS) variables indicates that FAW distribution occurs in an aggregate way (Gireesh et al., 2021), being possible to observe areas of higher incidence or severity. These areas are the points of monoculture establishments (negative control) that did not receive treatment to control the pest (green areas of Figures 7 and 8).

The soil moisture (Mohanty et al., 2000; Karamouz et al., 2021) and temperature data (Teixeira et al., 2012) were better fitted to the Gaussian model. This suggests that both variables present a regular and continuous spatial distribution (Teixeira et al., 2012). The lowest values of the selection criteria were recorded in the Gaussian model, which indicates a better fit of this to the experimental variograms of soil moisture and temperature (Table 5).

Fall armyworm incidence presented a strong spatial dependence in the first 2 wk and a moderate one in the third week (FAI3) (Table 4). This result agrees with Farias et al. (2008), according to which FAW spatial dependence decreases with the development of its population until it becomes random. In this study, this state was not reached because of the effects of the different management systems on the pest population. Even FAW severity at the third week (FAS) showed a strong spatial dependence. On the other hand, the edaphoclimatic variables presented a moderate spatial dependence.

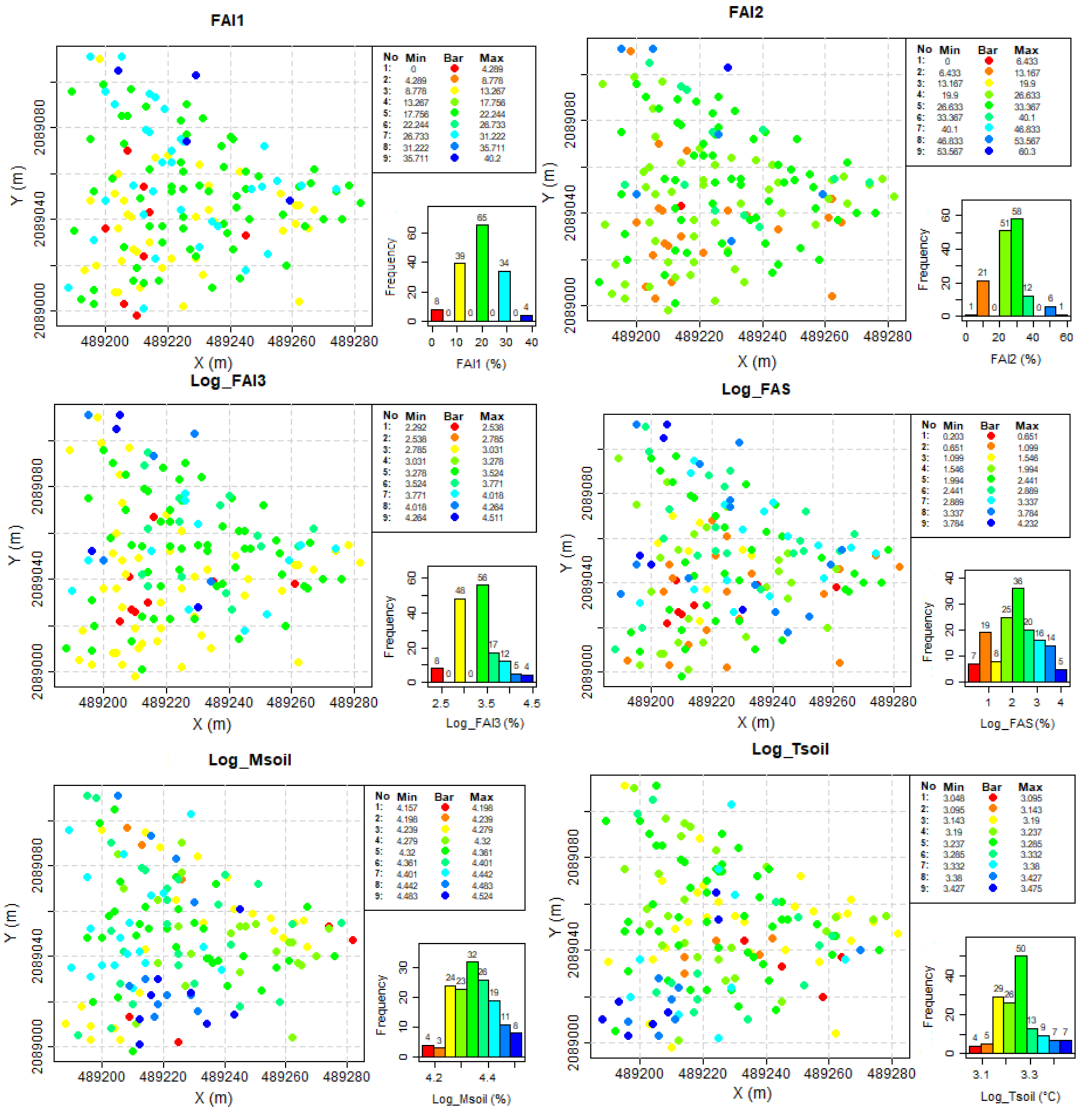

Figure 3. Spatial distribution of soil moisture and temperature and fall armyworm (FAW) incidence and severity in the mosaic of systems established in Yautepec, Morelos, México. FAI1: FAW incidence at 7 d; FAI2: FAW incidence at 14 d; FAI3: FAW incidence at 21 d; FAS: FAW severity at 21 d; Msoil: soil moisture; Tsoil: soil temperature.

Table 4. Estimates of the parameters of the theoretical semivariogram models. C_0: Nugget effect; $C_0 + C_1$: sill; R: range; DSD: degree of spatial dependence; FAI1: fall armyworm (FAW) incidence at 7 d; FAI2: FAW incidence at 14 d; FAI3: FAW incidence at 21 d; FAS: FAW severity at 21 d; Msoil: soil moisture; Tsoil: soil temperature.

Variables	Model	C_0	$C_0 + C_1$	R(m)	DSD (%)
FAI1	Spherical	10	78	16	12.821
FAI2	Spherical	10	99	16	10.101
Ln (FAI3)	Spherical	0.06	0.19	16	31.579
Ln (FAS)	Spherical	0.15	0.90	16	16.667
Ln (Msoil)	Gaussian	0.0115	0.020	25	57.500
Ln (Tsoil)	Gaussian	0.0047	0.0105	25	44.762

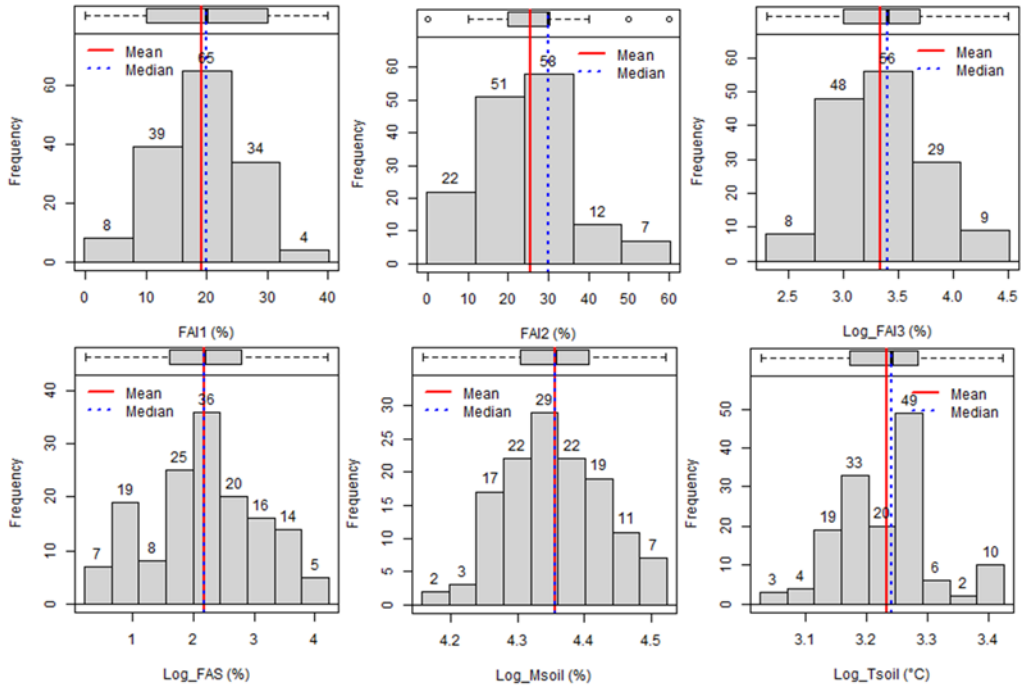

Figure 4. Histograms and boxplots of fall armyworm (FAW) incidence (at 7, 14 and 21 d), FAW severity (at 21 d), soil moisture (without 18 outliers) and soil temperature (without 4 outliers) in push-pull systems established in Morelos, Mexico. FAI1: FAW incidence at 7 d; FAI2: FAW incidence at 14 d; FAI3: FAW incidence at 21 d; FAS: FAW severity at 21 d; Msoil: soil moisture; Tsoil: soil temperature.

Spatial estimation

Thematic maps of the spatial distribution of FAW incidence and severity and soil temperature and moisture are found in Figures 7, 8, and 9, respectively. Fall armyworm incidence evolution over the 3 wk is perceptible, reaching high levels (green areas) in the monoculture establishment points in the third week. These points also coincide with greater FAW severity (Figure 8).

These results align with Hernández-Mendoza et al. (2008): FAW lower densities present an aggregated spatial distribution, while the higher densities have a random and uniform distribution. This trend does not occur in an

absolute way since studies such as those by Ríos et al. (2014) reported this aggregate distribution pattern, both for small and large fall armyworm larvae, both in early and advanced infestation stages.

In this study, an evolution of FAW incidence distribution is effectively observed, going from a more aggregated one in the first week when the insects were beginning to colonize the area, to a less aggregated and more random one in the third week. The distribution does not become random because of the repellent plants of the push-pull systems. These plants reduced FAW migration from highly infested monocultures to push-pull systems, which presented lower levels of damage. Therefore, a relatively aggregated distribution is still observed in the third week. The estimated spatial distributions for that last week indicated that FAW incidence in push-pull systems varied mostly between 10% and 40%, and in maize monocultures, between 35% and 90%.

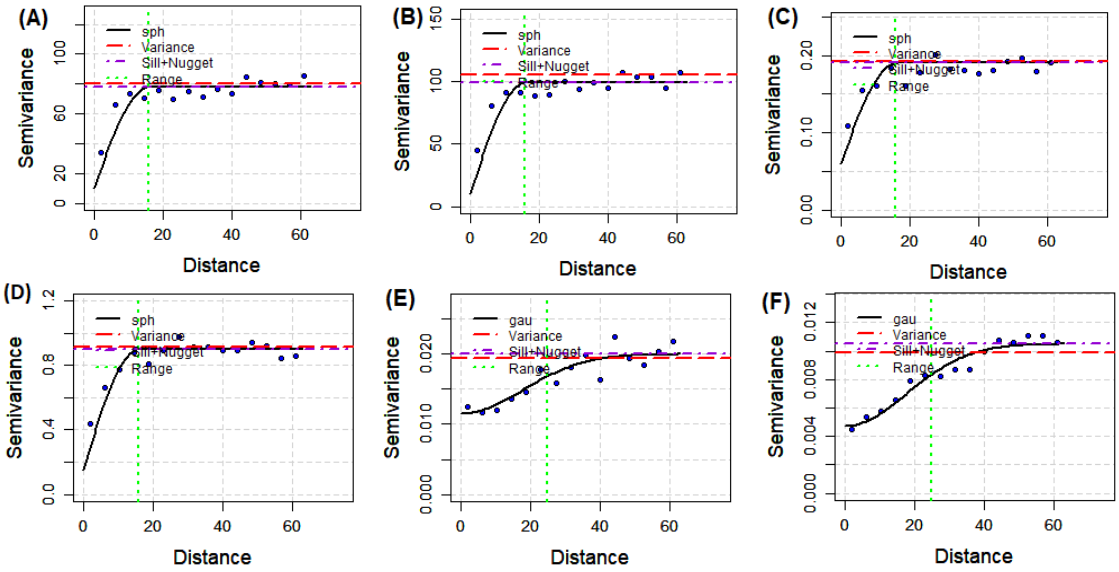

Figure 5. Variograms of incidence FAI1 (A), FAI2 (B), Ln (FAI3) (C) and severity Ln (FAS) (D) of fall armyworm and soil moisture Ln (Msoil) (E) and temperature Ln (Tsoil) (F).

Table 5. Models' selection criteria values. FAI1: Fall armyworm (FAW) incidence at 7 d; FAI2: FAW incidence at 14 d; FAI3: FAW incidence at 21 d; FAS: FAW severity at 21 d; Msoil: soil moisture; Tsoil: soil temperature; AICc: corrected Akaike information criterion; BIC: Bayesian information criterion; RMSE: root mean square error; MAE: mean absolute error.

Variables	Model	AICc	BIC	RMSE (%)	MAE
FAI1	Spherical	119.592	100.716	28.177	0.763
FAI2	Spherical	124.887	106.011	26.713	0.767
Ln (FAI3)	Spherical	-80.023	-98.898	15.686	0.002
Ln (FAS)	Spherical	-25.704	-44.579	19.756	0.044
Ln (Msoil)	Gaussian	-154.099	-172.975	14.257	-0.001
Ln (Tsoil)	Gaussian	-173.764	-192.640	14.535	-0.001

Table 6. Estimates of the parameters of the models adjusted to the cross variogram. VP: Primary variable; VS: secondary variable; C0: Nugget effect; C0 + C1: sill; R: range; DSD: degree of spatial dependence; FAI3: fall armyworm (FAW) incidence at 21 d; FAS: FAW severity at 21 d; Msoil: soil moisture; Tsoil: soil temperature.

VP/VS	Model	C_0	$C_0 + C_1$	R(m)	DSD (%)
Ln(FAS)/Ln(FAI3)	Spherical	0.0500	0.350	16	14.286
Ln(Msoil)/Ln(Tsoil)	Gaussian	0.0025	0.006	25	41.667

The FAW damage severity ranged between 20% and 70% in monocultures and between 1% and 25% in the push-pull systems. These results confirm that FAW distribution in an agroecosystem depends, among other factors, on its agroecological conditions and the plant species that constitutes it (Hernández-Mendoza et al., 2008).

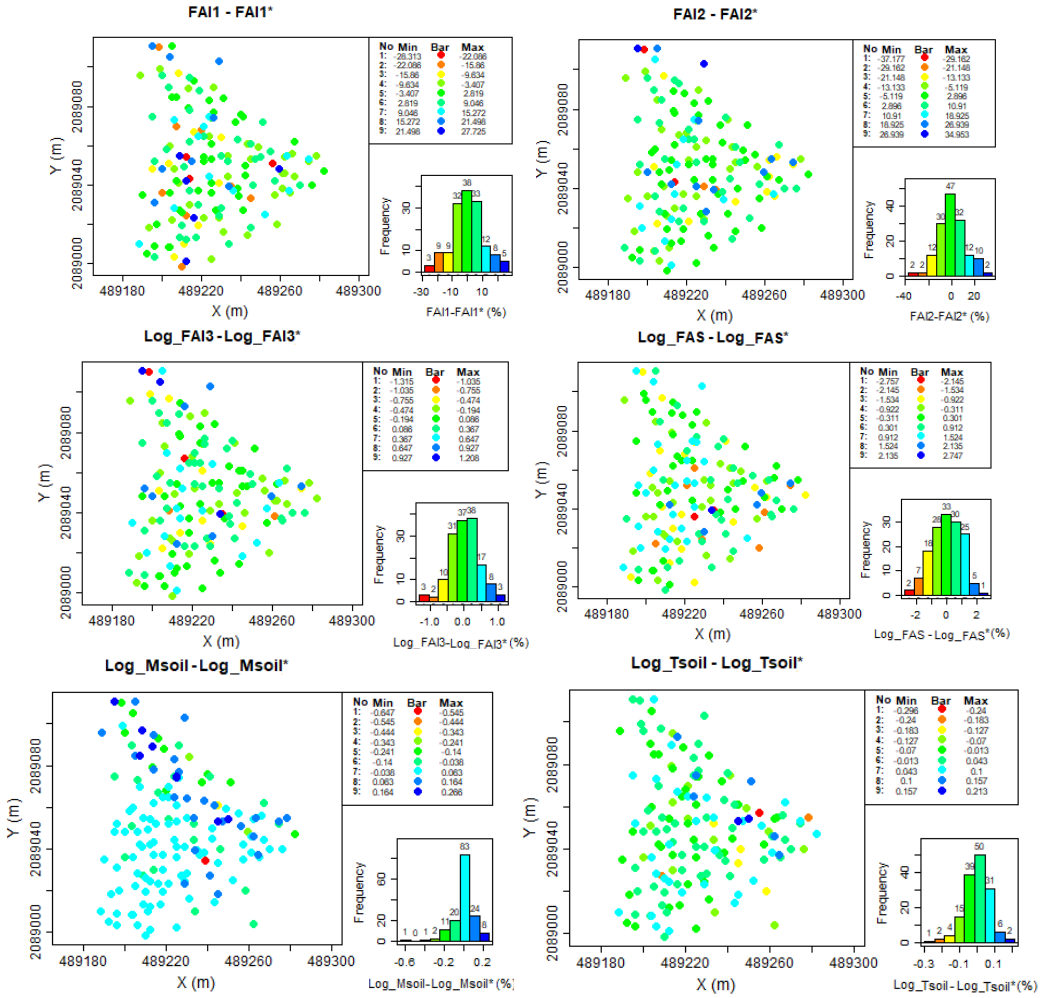

Figure 6. Distributions and histograms of the normalized errors of the fitted model. FAI1: Fall armyworm (FAW) incidence at 7 d; FAI2: FAW incidence at 14 d; FAI3: FAW incidence at 21 d; FAS: FAW severity at 21 d; Msoil: soil moisture; Tsoil: soil temperature.

Table 7. Models' selection criteria values for the models fitted to the cross variogram. VP: Primary variable; VS: secondary variable; AICc: corrected Akaike information criterion; BIC: Bayesian information criterion; RMSE: root mean square error; MAE: mean absolute error; FAI3: fall armyworm (FAW) incidence at 21 d; FAS: FAW severity at 21 d; Msoil: soil moisture; Tsoil: soil temperature.

VP/VS	Model	AICc	BIC	RMSE (%)	MAE
Ln(FAS)/Ln(FAI3)	Spherical	-57.515	-76.391	17.883	1.057E-02
Ln(Msoil)/Ln(Tsoil)	Gaussian	-180.255	-199.131	21.485	-6.495E-04

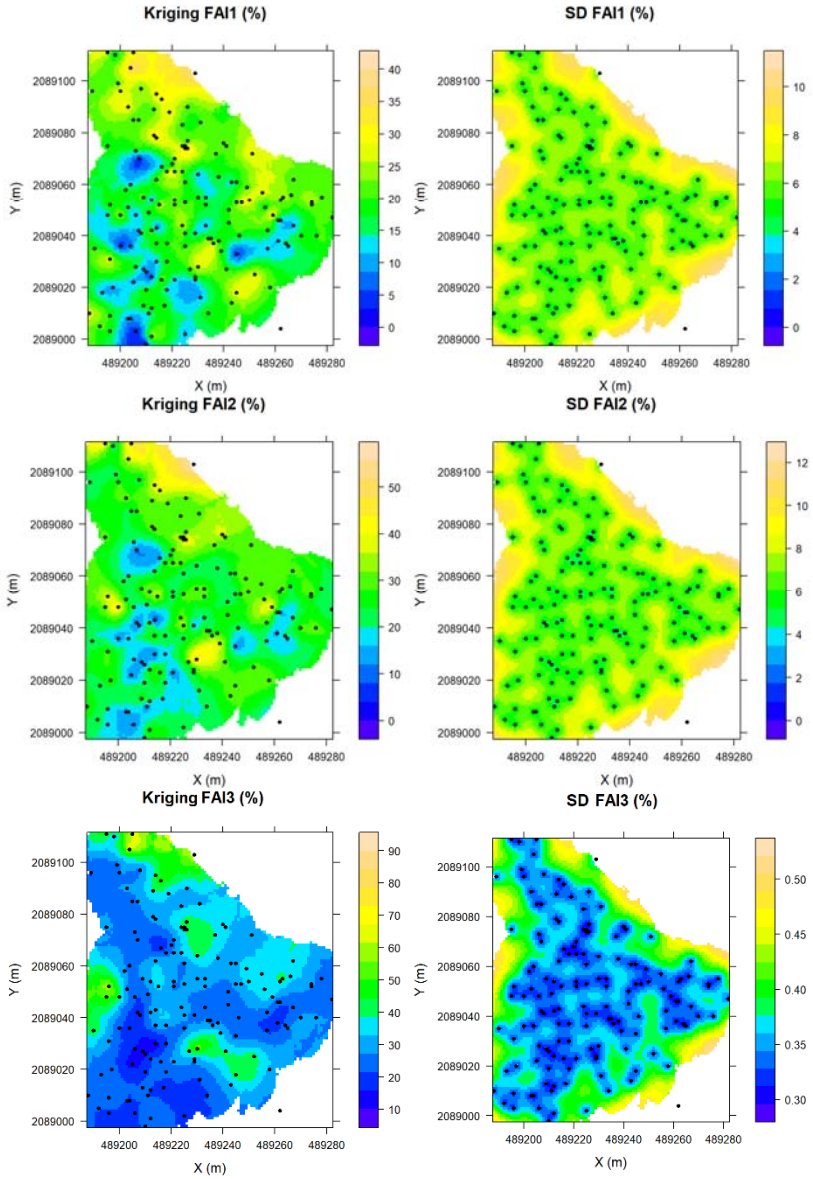

Figure 7. Ordinary kriging maps for fall armyworm (FAW) incidence in the first 3 wk (estimates maps on the left and error maps on the right). FAI1: FAW incidence at 7 d; FAI2: FAW incidence at 14 d; FAI3: FAW incidence at 21 d.

Maps confirm that soil moisture and temperature follow a regular and uniform distribution (Figure 9). It was impossible to associate the observed distribution pattern with the different systems that constitute the agroecosystem mosaic. In part, this is because water management was not prioritized in the design of the systems and, on the other hand, the number of factors on which the edaphoclimatic variables depend. The main factors contributing to soil moisture variability at different spatial scales and timescales are soil properties, topography, vegetation, land management, precipitation, and temperature (Mohanty et al., 2000).

Multivariate geostatistics to assess patterns of spatial dependence of FAW severity and soil moisture

Cross variogram estimation. The FAW severity (FAS) is the most associated with maize yield, and soil moisture (Msoil) conservation is most associated with agroecosystems sustainability. The variables most correlated with these are FAW incidence at the third week (FAI3) and soil temperature (Tsoil), respectively (Figure 2). Therefore, the primary variables (FAS and Msoil) were modeled with the secondary variables FAI3 and Tsoil, respectively.

Since the co-kriging was performed with two variables, three simple variograms were necessary. A variogram for the primary variable, another for the secondary variable, and a cross-variogram between both variables (Figure 10). The matrices of the linear coregionalization models were positive semi-definite.

Parameters estimates of the models fitted to the cross variograms are found in Table 6 and Figure 10 and evaluation criteria in Table 7. Except for root mean square error (RMSE), these criteria indicate a better fit of the Msoil variographic model, generating more accurate and less biased estimates than the FAS model.

The error maps (Z - Z*) obtained from the LOOCV of the models are found in Figure 11. These, like the previous variograms, indicate mean errors close to zero (Table 7), which indicate that the fitted models generate unbiased estimates.

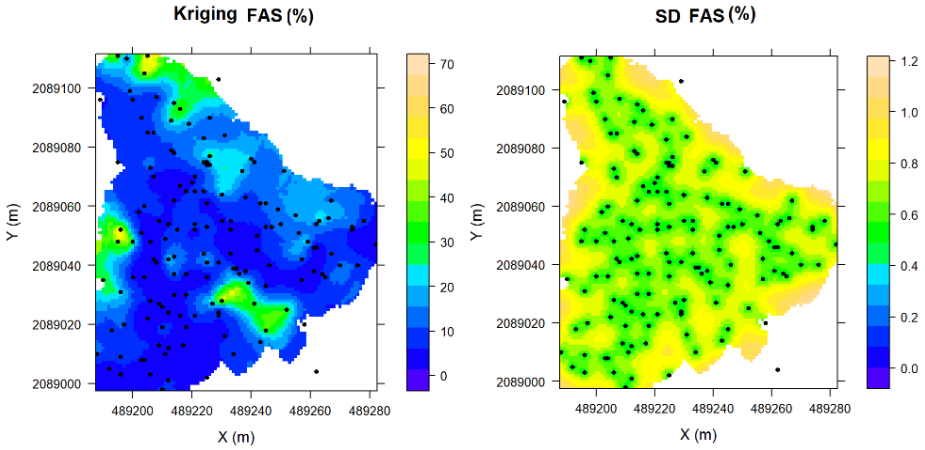

Figure 8. Ordinary kriging maps for fall armyworm (FAW) severity at the third week (FAS) of maize crop (estimates map on the left and error map on the right).

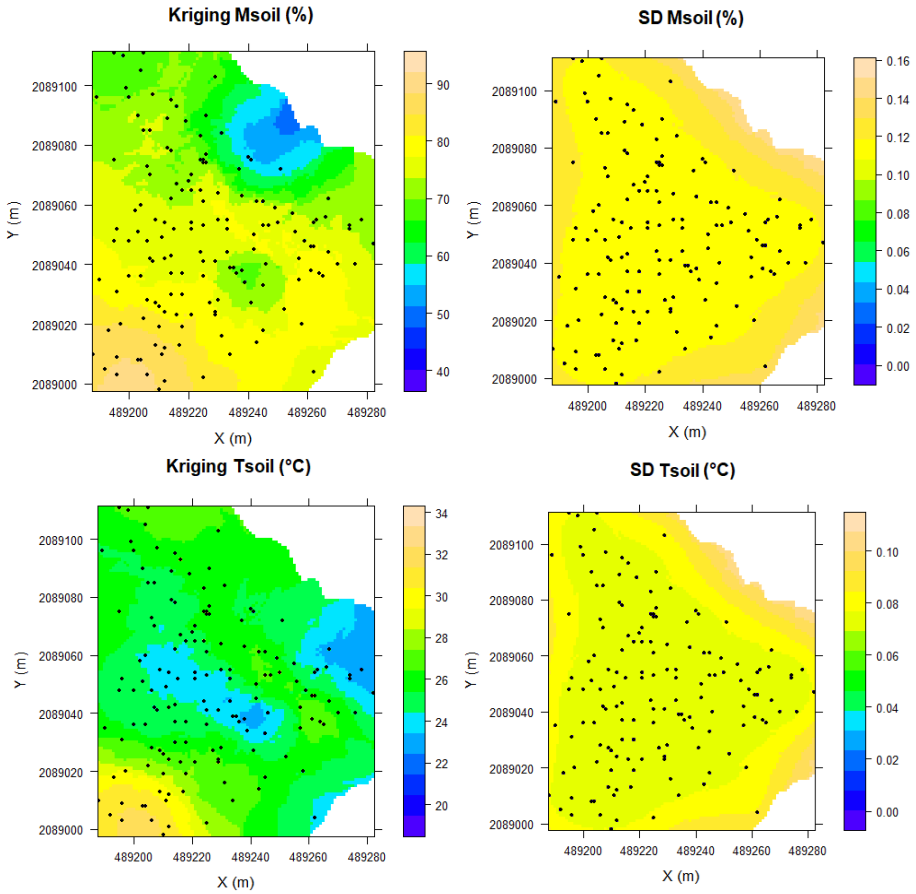

Figure 9. Ordinary kriging maps for soil moisture (Msoil) and temperature (Tsoil) after vegetative development of maize crops (estimates maps on the left and error maps on the right).

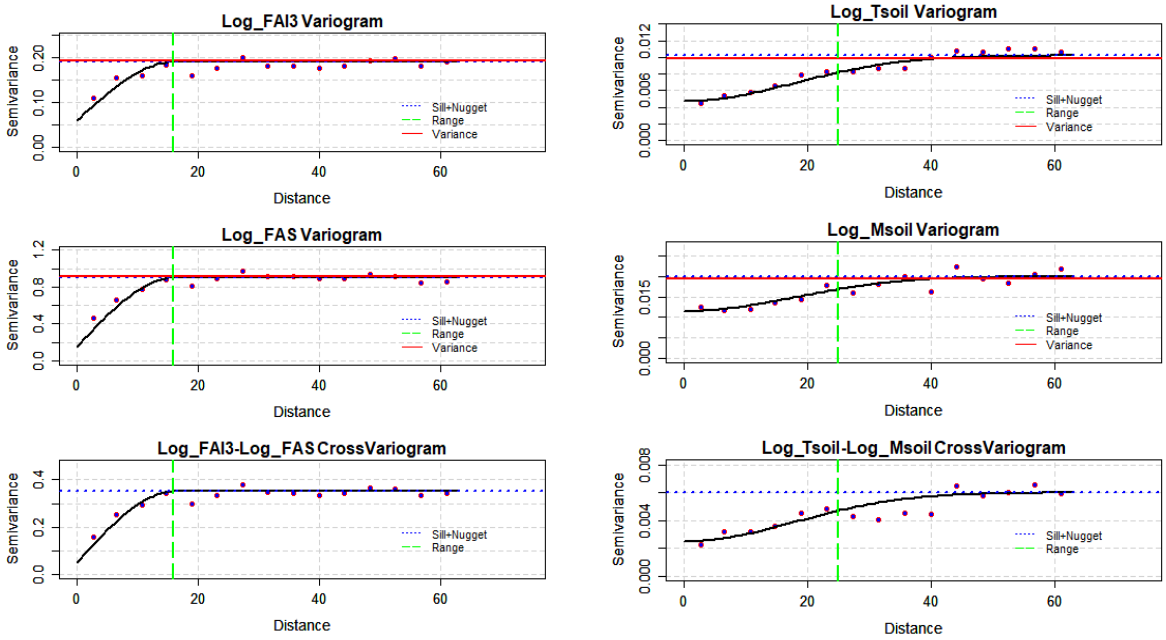

Figure 10. Fall armyworm severity (FAS) and soil moisture (Msoil) cross variograms.

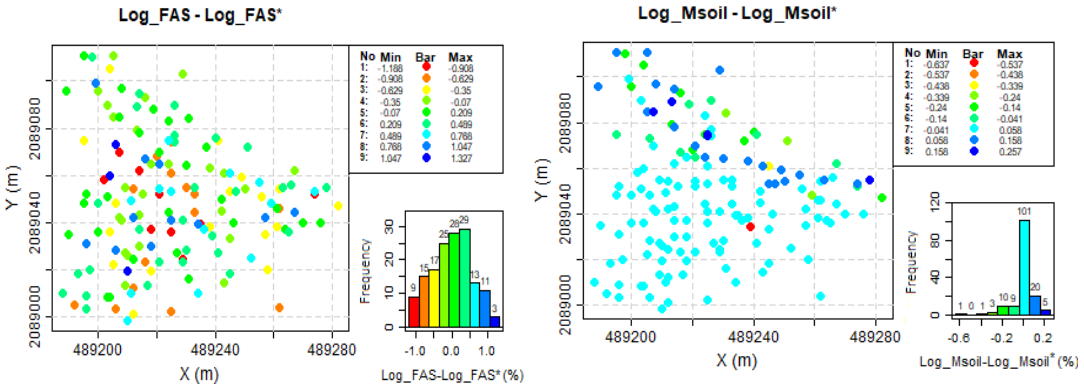

Figure 11. Distributions and histograms of the normalized errors of the models fitted to the cross variograms of fall armyworm severity (FAS) and soil moisture (Msoil).

Spatial estimation by cokriging. Maps of spatial estimates of FAS and Msoil by cokriging are presented in Figures 12 and 13, respectively. The interpolations by cokriging, both for FAS and Msoil, presented distribution patterns like those obtained by kriging. In addition, these interpolations are more accurate and less biased (MAEcokriging < MAEkriging) than those obtained by the kriging method, this being one of the advantages of cokriging, especially when the variables under study are cross-correlated (Isaaks and Srivastava, 1989).
Geostatistical techniques allowed the analysis of FAW distribution patterns to understand its dynamics during the greatest vulnerability of maize crops (first 3 wk). The main limitation of this study is that it does not allow us to analyze the effect of each push-pull system on FAW spatiotemporal dynamics. In fact, the study did not set this objective because it would imply performing the geostatistical analyzes by the system, which was not possible due to insufficient data. Kerry and Oliver (2008), among other authors, recommend that a minimum of 100 to 150 points be used to construct reliable variograms. The size of each agroecosystem was 196 m^2 (14 m × 14 m plots). Of this, 100 m^2 (10 m × 10 m) were planted with maize except for the monoculture. It is an area considered small to meet the sample requirements. Therefore, the study was carried out considering the entire mosaic of agroecosystems. Five samples in each of the 30 agroecosystems that constitute this mosaic total the 150 points recommended for obtaining a reliable variogram.

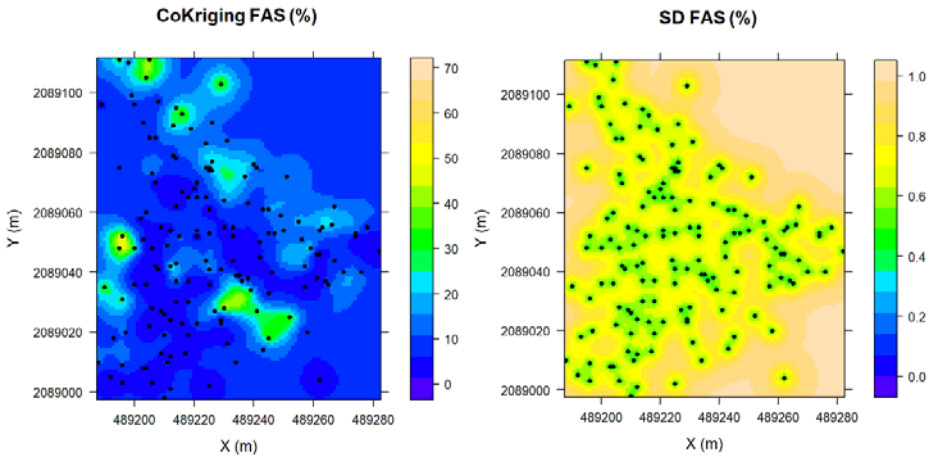

Figure 12. Ordinary cokriging maps for fall armyworm severity (FAS) at the third week of maize crops.

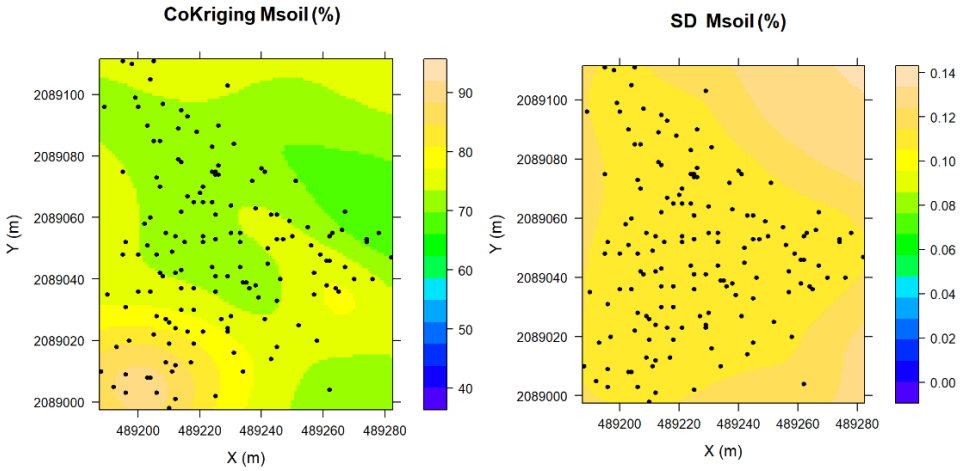

Figure 13. Ordinary cokriging maps for soil moisture (Msoil) after vegetative development of maize crops.

CONCLUSIONS

The phytosanitary variables presented a strong spatial dependence and the edaphoclimatic variables a moderate one. Soil temperature and moisture presented a continuous and more uniform spatial distribution. Fall armyworm incidence and severity presented an aggregated spatial distribution, with monocultures as the main foci of infestation. Identifying these foci, made possible by the aggregated distribution pattern, improves the efficiency of pest control methods, such as mass trapping, mating disruption, and release of natural enemies, among others.

Author contributions

Conceptualization: O.G.M.G., F.C.-A., N.R. Methodology: O.G.M.G., F.C.-A., N.R. Validation: F.C.-A., N.R., A.J.-P., M.A.D.-V., J.A.A.dS. Formal analysis: O.G.M.G., V.-H.L. Investigation: O.G.M.G. Resources: F.C.-A., N.R. Data curation: O.G.M.G. Writing-original draft preparation: O.G.M.G. Writing-review and editing: O.G.M.G., F.C.-A., N.R., A.J.-P., V.-H.L., M.A.D.-V., J.A.A.dS. Supervision: F.C.-A., N.R. Project administration: F.C.-A. Funding acquisition: F.C.-A., N.R. All authors have read and agreed to the published version of the manuscript.

Acknowledgements

The authors thank: CONACYT for the scholarship for doctoral studies awarded to the first author, SIP-IPN (Projects SIP 2019-5544 and SIP 2019-4962), the Biotic Products Development Center of the National Polytechnic Institute (CEPROBI-IPN), the International Maize and Wheat Improvement Center (CIMMYT) and the National Institute for Forestry, Agriculture and Livestock Research (INIFAP). We also thank Agustin Miranda for the loan of the experimental area and logistical support during the experiment. Finally, we thank the master's students in Agroecological Management of Pests and Diseases of CEPROBI-IPN (Generation B-2018) for their support during the arduous field work, from the establishment of the experiment to the harvest.

References

Al-Kayssi, A.W., Al-Karaghouli, A.A., Hasson, A.M., Beker, S.A. 1990. Influence of soil moisture content on soil temperature and heat storage under greenhouse conditions. Journal of Agricultural Engineering Research 45:241-252. doi:10.1016/S0021-8634(05)80152-0.

Azizan, F.A., Zalani, F.N.M., Nagarajan, A., Aznan, A.A., Ruslan, R. 2019. Analysis of spatial distribution of soil moisture content for different soil layers in mango greenhouse. IOP Conference Series: Materials Science and Engineering 557:012070.

Bebber, D.P., Ramotowski, M.A.T., Gurr, S.J. 2013. Crop pests and pathogens move polewards in a warming world. Nature Climate Change 3(11):985-988. doi:10.1038/nclimate1990.

Box, G.E.P., Cox, D.R. 1964. An analysis of transformations. Journal of the Royal Statistical Society. Series B (Methodological) 26(2):211-252.

Brevik, E.C., Calzolari, C., Miller, B.A., Pereira, P., Kabala, C., Baumgarten, A., et al. 2016. Soil mapping, classification, and pedologic modeling: History and future directions. Geoderma 264:256-274. doi:10.1016/j.geoderma.2015.05.017.

Cambardella, C.A., Moorman, T.B., Novak, J.M., Parkin, T.B., Karlen, D.L., Turco, R.F., et al. 1994. Field-scale variability of soil properties in Central Iowa Soils. Soil Science Society of America Journal 58(5):1501-1511. doi:10.2136/sssaj1994.03615995005800050033x.

Chilès, J.P., Delfiner, P. 2012. Geostatistics, modeling spatial uncertainty. 2nd ed. Wiley Series in Probability and Statistics. John Wiley & Sons, New York, USA.

Cressie, N. 1993. Statistics for spatial data. John Wiley, New York, USA.

Davis, P.M. 1994. Statistics for describing populations. p. 33-54. In Pedigo, L., Buntin, G.D. (eds.) Handbook of sampling methods for arthropods in agriculture. CRC Press, Florida, USA.

Díaz-Viera, M.A., Hernández-Maldonado, V., Méndez-Venegas, J., Mendoza-Torres, F., Le, V.H., Vázquez-Ramírez, D. 2021. RGEOESTAD: Un programa de código abierto para aplicaciones geoestadísticas basado en R-Project. Available at http://www.esmg-mx.org/activities/courses/geoestadistica.

Dminić, I., Kozina, A., Bažok, R., Barčić, J.I. 2010. Geographic information systems (GIS) and entomological research: A review. Journal of Food, Agriculture & Environment 8(2):1193-1198.

Famiglietti, J.S., Rudnicki, J.W., Rodell, M. 1998. Variability in surface moisture content along a hillslope transect: Rattiesnake Hill, Texas. Journal of Hydrology 210(1-4):259-281. doi:10.1016/s0022-1694(98)00187-5.

Farias, P.R.S., Barbosa, J.C., Busoli, A.C., Overal, W.L., Miranda, V.S., Ribeiro, S.M. 2008. Spatial analysis of the distribution of *Spodoptera frugiperda* (Lepidoptera: Noctuidae) and losses in maize crop productivity using geostatistics. Neotropical Entomology 37(3):321-327. doi:10.1590/S1519-566X2008000300012.

Gireesh, M., Rijal, J.P., Joseph, S.V. 2021. Spatial distribution of hunting billbugs (Coleoptera: Curculionidae) in sod farms. Insects 12(5):1-14. doi:10.3390/insects12050402.

Gosselin, A., Trudel, M.J. 1986. Root-zone temperature effects on pepper. Journal of the American Society for Horticultural Science 2:220-224.

Goovaerts, P., Chiang, C. 1993. Temporal persistence of spatial patterns for mineralizable nitrogen and selected soil properties. Soil Science Society of America Journal 57(2):372-381. doi:10.2136/sssaj1993.03615995005700020015x.

Guera, O.G.M., Castrejón-Ayala, F., Robledo, N., Jiménez-Pérez, A., Sánchez-Rivera, G. 2020. Plant selection for the establishment of push-pull strategies for *Zea mays*-*Spodoptera frugiperda* pathosystem in Morelos, Mexico. Insects 11(6):1-23. doi:10.3390/insects11060349.

Guera, O.G.M., Castrejón-Ayala, F., Robledo, N., Jiménez-Pérez, A., Sánchez-Rivera, G., Salazar-Marcial, L., et al. 2021. Effectiveness of push-pull systems to fall armyworm (*Spodoptera frugiperda*) management in maize crops in Morelos, Mexico. Insects 12(4):1-15. doi:10.3390/insects12040298.

Hernández-Mendoza, J.L., López-Barbosa, E.C., Garza-González, E., Mayek-Pérez, N. 2008. Spatial distribution of *Spodoptera frugiperda* (Lepidoptera: Noctuidae) in maize landraces grown in Colima, Mexico. International Journal of Tropical Insect Science 28(3):126-129. doi:10.1017/S1742758408096112.

Hutasoit, R.T., Kalqutny, S.H., Widiarta, N. 2020. Spatial distribution pattern, bionomic, and demographic parameters of a new invasive species of armyworm *Spodoptera frugiperda* (Lepidoptera; Noctuidae) in maize of South Sumatra, Indonesia. BIODIVERSITAS 21(8):3576-3582. doi:10.13057/biodiv/d210821.

Isaaks, E., Srivastava, M. 1989. Applied geostatistics. Oxford University Press, New York, USA.

Karamouz, M., Ebrahimi, E., and Ghomlaghi, A. 2021. Soil moisture data using citizen science technology cross-validated by satellite data. Journal of Hydroinformatics 23(6):1224-1246. doi:10.2166/hydro.2021.029.

Kerry, R., Oliver, M.A. 2008. Determining nugget: sill ratios of standardized variograms from aerial photographs to krige sparse soil data. Precision Agriculture 9:33-56. doi:10.1007/s11119-008-9058-0.

Liebhold, A.M., Rossi, R.E., Kemp, W.P. 1993. Geostatistics and geographic information systems in applied insect ecology. Annual Review of Entomology 38:303-327. doi:10.1146/annurev.en.38.010193.001511.

Lopes, I., Montenegro, A.A.A. 2019. Space dependence of soil moisture and soil electrical conductivity in alluvial region. IRRIGA 24(1):1-15. doi:10.15809/irriga.2019v24n1p1-15.

Matheron, G. 1963. Principles of geostatistics. Economic Geology 58(8):1246-1266. doi:10.2113/gsecongeo.58.8.1246.

Mohanty, B.P., Famiglietti, J.S., Skaggs, T.H. 2000. Evolution of soil moisture spatial structure in a mixed vegetation pixel during the Southern Great Plains 1997 (SGP97) Hydrology Experiment. Water Resources Research 36(12):3675-3686.

Montezano, D.G., Specht, A., Sosa-Gómez, D.R., Roque-Specht, V.F., Sousa-Silva, J.C., Paula-Moraes, S.V., et al. 2018. Host plants of *Spodoptera frugiperda* (Lepidoptera: Noctuidae) in the Americas. African Entomology 26(2):286-300. doi:10.4001/003.026.0286.

Oliver, M.A. 2010. Geostatistical applications for precision agriculture. Springer, Dordrecht, Netherlands.

Prá, E.D., Guedes, J.V.C., Cherman, M.A., Jung, A.H., Silva, S.J.P., Ribas, G.G. 2011. Uso da geoestatística para caracterização da distribuição espacial de larvas de *Diloboderus abderus*. Ciência Rural 41(10):1689-1694. doi:10.1590/S0103-84782011001000002.

Pringle, M.J., Bishop, T.F.A., Lark, R.M., Whelan, B.M., McBratney, A.B. 2010. The analysis of spatial experiments. p. 243-265. In Oliver, M.A. (ed.) Geostatistical applications for precision agriculture. Springer, Dordrecht, Netherlands.

Ramírez-Dávila, J.F., González, J.L., Ocete, R., López, M.A. 2002. Descripción geoestadística de la distribución espacial de los huevos del mosquito verde *Jacobiasca lybica* (Bergenin & Zanon) (Homoptera: Cicadellidae) en viñedo: modelización y mapeo. Boletín de sanidad vegetal. Plagas 28(1):87-95.

Ríos, E.S., Martins, I.C.F., Noronha, M.P., Silva, J.A., Filho, J.G.S., Badji, C.A. 2014. Spatial distribution of *Spodoptera frugiperda* in the wasteland of southern Pernambuco state, Brazil. Revista de Ciências Agrárias-Amazonian Journal of Agricultural and Environmental Sciences 57(3):297-304. doi:10.4322/rca.ao1461.

Talchabhadel, R., Karki, R., Yadav, M., Maharjan, M., Aryal, A., Raj, T.B. 2019. Spatial distribution of soil moisture index across Nepal: a step towards sharing climatic information for agricultural sector. Theoretical and Applied Climatology 137(3-4):3089-3102. doi:10.1007/s00704-019-02801-3.

Teixeira, D.B., Bicalho, E.S., Panosso, A.R., Perillo, L.I., Iamaguti, J.L., Pereira, G.T., et al. 2012. Uncertainties in the prediction of spatial variability of soil CO_2 emissions and related properties. Revista Brasileira de Ciência do Solo 36(5):1466-1475. doi:10.1590/S0100-06832012000500010.

Zhang, Z., Pan, Z., Pan, F., Zhang, J., Han, G., Huang, N., et al. 2020. The change characteristics and interactions of soil moisture and temperature in the farmland in Wuchuan County, Inner Mongolia, China. Atmosphere 11(5):1-14. doi:10.3390/atmos11050503.